

Direct Transition Phenomena in Pool Boiling of FC-72*

Purwono F. SUTOPO**, Katsuya FUKUDA** and Qiusheng LIU**

**Graduate School of Maritime Sciences, Kobe University

5-1-1, Fukaeminami, Higashinada, Kobe, 658-0022, Japan

E-mail: fukuda@maritime.kobe-u.ac.jp

Abstract

The direct transition boiling process from non-boiling to film boiling at critical heat flux (CHF) by exponentially increasing heat input, $Q_0 \exp(t/\tau)$, was investigated in a pool of FC-72. Investigations were made on a 1.0 mm diameter gold horizontal cylinder heater under a wide range of system pressures for saturated condition. Direct transition predominantly occurs from heat conduction process in the non-boiling regime by rapid increasing heat input and then followed by incipient boiling and CHF simultaneously. However, during quasi-steady-state heat transfer, it was observed that the direct transition also occurs from single phase natural convection at around atmospheric pressure and by an extent of pre-pressure, which was given to the cylinder surface at atmospheric pressure. Direct transition phenomena were confirmed to exist due to the explosive-like heterogeneous spontaneous nucleation (HSN) in originally flooded cavities on surface. The predictions of direct transition phenomena were also derived from typical incipient boiling superheat and CHF.

Key words: Transient, Direct Transition, CHF, Pre-pressure, FC-72

1. Introduction

Clarification of transition boiling process to film boiling at CHF in the pool boiling heat transfer is important for the development of fundamental knowledge and will be responsible for correct understanding its phenomena required for design and safety evaluation of heat generation system. The CHF for the transition boiling process represents an important limit of highly efficient heat transfer process. Increasing of heat flux over this limit may lead into burnout and system will suffer an excessive damaging increase in temperature.

The generalized types of transition process to film boiling from single-phase convection or transient conduction and fully or insufficiently developed nucleate boiling by a wide range of increasing heat inputs have been investigated in non-wetting and wetting liquids by several authors. In some liquids that have low surface tension such as liquid nitrogen and ethanol, ones observed direct transitions to film boiling without nucleate boiling from natural convection regime by a quasi-steadily increasing heat input at around atmospheric pressure and from transient conduction regime by increasing heat input at higher pressure⁽¹⁻³⁾. The incipient boiling is followed simultaneously by burnout attaining maximum heat flux and then proceeds to the transition boiling and steady state film boiling. The transition surface superheat for the direct transition at CHF is considerably lower than the corresponding homogeneous nucleation temperature.

They also suggested that the CHF from non-boiling heat transfer process and direct transition to film boiling could not be described by the conventional correlation for the CHF from fully developed nucleate boiling (FDNB) based on the hydrodynamic instability (HI).

*Received 19 May, 2010 (No. 10-0214)

[DOI: 10.1299/jtst.5.206]

Copyright © 2010 by JSME

It was assumed that the direct transition would occur due to the levitation of liquid from cylinder surface by the explosive-like HSN in originally flooded cavities without contribution of active cavities entraining vapors for boiling incipience. All cavities on the surface that could serve as nucleation sites would initially be flooded since there is no dissolved gas in liquid nitrogen and the liquid surface tension is so low that vapors are not entrained in surface cavities.

Prediction of pool boiling CHF by exponentially increasing heat inputs for period, τ , was suggested early by Sakurai and Shiotsu⁽⁴⁾, which took account the heat transfer coefficient from transient non-boiling regime of conduction process. Studies of the boiling heat transfer including explosive boiling induced by spontaneous nucleation close to its superheat limit by transient heating were also formerly done by several researchers⁽⁵⁻⁷⁾. They observed the dynamics of boiling such that the incipient boiling process was dominated by spontaneous nucleation. One observed also that the transient incipient boiling process was time dependence by heterogeneous nucleation process⁽⁸⁾.

Pool boiling in highly wetting liquid of FC-72 by transient heat inputs has been also investigated by authors and the others⁽⁹⁻¹⁴⁾. Recently, experimental investigations in the pool boiling of FC-72 on finite horizontal heaters by exponentially increasing heat inputs were performed to investigate the boiling phenomena and the steady-state and transient critical heat fluxes under a wide range of pressures and liquid subcoolings⁽⁹⁻¹²⁾. The current work investigated the direct transition process from non-boiling to film boiling in a pool of saturated fluorinert FC-72 under a wide range of pressures by exponentially increasing heat inputs from quasi-steady-state to rapid ones to observe the boiling phenomena including the incipient boiling process and the corresponding CHF. In this work, 292 known data from measurements on the cylinder heater at saturated condition were analyzed and presented.

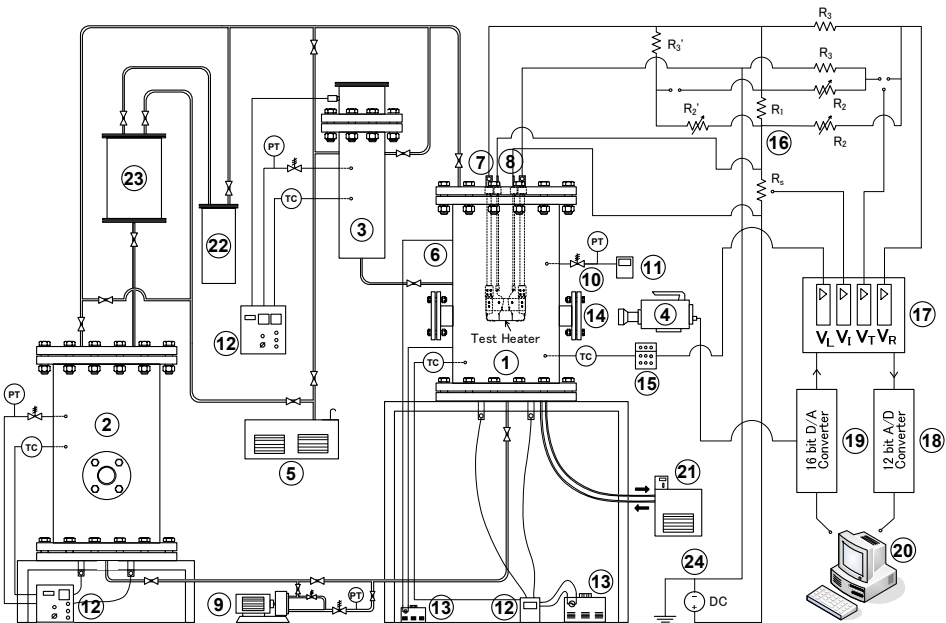
2. Nomenclature

A	constant in Eq. (6a)
a	$(\lambda/\rho_h c_{ph})$, thermal diffusivity, m^2/s
B	constant in Eq. (6b)
c_p	specific heat at constant pressure, J/kgK
d	cylinder diameter, m
h_c	heat transfer coefficient by transient heat conduction, W/m^2K
k	thermal conductivity, W/mK
P	pressure, Pa
P/P_{CR}	reduced pressure, where $P_{CR} = 1830$ kPa
Q	heat generation rate, W/m^3
Q_0	initial heat generation rate, W/m^3
q	heat flux, W/m^2
q_c	CHF, W/m^2
q_i	incipient boiling heat flux, W/m^2
r	cylinder radius, m ; radius of vapor embryo, m
T	temperature of the test heater, K
T_a	average temperature of the test heater, K
T_{CR}	critical temperature of FC-72 = 450 K
T_H	homogeneous nucleation temperature, K
T_{sat}	saturation temperature, K
T_{sp}	spinodal limit temperature, K
T_w	heater surface temperature, K
ΔT_i	incipient boiling surface superheat, K

ΔT_{sat}	$(T_w - T_{sat})_t$, surface superheat, K
t	time, s
σ	surface tension, N/m
λ	thermal conductivity, W/mK
ρ	density, kg/m ³
τ	exponential period, s

Subscripts

h	heater
l	liquid
v	vapor



- | | | |
|-----------------------------|-----------------------------|--------------------------|
| (1) Boiling vessel | (9) Booster pump | (17) Heat control system |
| (2) Auxiliary tank | (10) Pressure relief valve | (18) A/D converter |
| (3) Pressurizer | (11) Pressure gauge | (19) D/A converter |
| (4) High-speed video camera | (12) Temperature controller | (20) PC |
| (5) Vacuum pump | (13) Slide rheostat | (21) Tube cooler |
| (6) Micro heater | (14) Observation window | (22) Condenser |
| (7) Current conductor | (15) Cold junction | (23) Receiver tank |
| (8) Potential conductor | (16) Bridge circuit | (24) DC power supply |

Fig. 1. Pool boiling experimental apparatus

Table 1. Specification parameters of test section

Geometry	Cylinder	
Material	Gold	
Spot distance from terminal	15.0 mm	
Effective length	54.7 mm	
Diameter	1.0 mm	

3. Experimental Method and Apparatus

3.1 Experimental apparatus and test section

The representation drawing of the pool boiling experimental apparatus is shown in Fig. 1, which was developed by Sakurai and Shiotsu⁽⁴⁾. The test chamber or boiling vessel with observation windows is made of stainless steel with 200 mm of inner diameter and 600 mm in height. The vessel is designed for an application of pressure up to 2 MPa. Two current conductors and two potential conductors are mounted at the upper side of the vessel. The liquid temperature in the boiling vessel is heated by a sheathed heater installed at downside of the vessel. The vessel is kept warm by micro heaters and thermally isolated with lagging materials. The liquid temperature in boiling vessel is measured by K-type thermocouples. A pressure transducer to measure the system pressure inside vessel is equipped with a pressure relief valve.

As seen in Fig. 1, the test section or test heater is mounted horizontally inside the boiling vessel. In this study, a finite gold horizontal cylinder with a diameter of 1.0 mm was used as the test section or heater. The specification parameters of heater are listed in Table 1. On the heater, two fine 50 μm diameter of wires were spot-welded on the heater surface as the potential taps. Thus, the effective length of test heater can be determined as the distance between the potential taps. The effective length of heater is 54.7 mm.

Heater was annealed in order to maintain the material at even properties, and the electrical resistance versus temperature relation was calibrated in water and glycerin baths using a precision double bridge circuit. The calibration accuracy was estimated to be within ± 0.5 K. All the material of test sections were applied as it is from the factory without any treatments or finishes on surface, and is often named as “Commercial Surface (CS)”. However, before they were mounted inside the boiling vessel, necessary cleaning on surface was taken to minimize any possible solid carbons or dirt.

3.2 Experimental method and procedure

The test heater was heated electrically by using a fast response, direct current source (max. 700 A) controlled by a digital computer so as to give increasing heat input with a period. The average temperature of the test heater was measured by resistance thermometry using the heater itself. A double bridge circuit with the heater as a branch was first balanced at the bulk liquid temperature. The output voltages of the bridge circuit, together with the voltage drops across the potential taps of the heater and across a standard resistance, were amplified and passed through analog-to-digital converters of a personal computer. These voltages were simultaneously sampled at a constant time interval. The fastest sampling speed of the A/D converter is 5 $\mu\text{s}/\text{channel}$. The average temperature was obtained by using the previously calibrated resistance-temperature relation.

The heat generation rate of the test heater was determined from the current to the heater and the voltage difference between potential taps on the test heaters. The surface temperature was obtained by solving the conduction equation in the heater under the conditions of the average temperature and heat generation rate. The instantaneous surface heat flux was obtained from the heat balance equation for a given heat generation rate. The experimental error was estimated to be about ± 1 K in the heater surface temperature and ± 2 % in the heat flux.

$$Q = Q_0 e^{t/\tau} \quad (1)$$

The electric current was supplied to the test heater, and the heat generation rate, Q , increased with exponential function. The heat input control system then controlled and measured the heat generation rate of the heater. The average temperature of test heater

was measured by resistance thermometry using a double bridge circuit including the test heater as a branch. The heat flux of the heater was calculated by the following equation for heat balance.

$$q = \frac{d}{4} \left(Q - \rho_h c_{ph} \frac{dT_a}{dt} \right) \quad (2)$$

The test heater surface temperature can be calculated from unsteady heat conduction equation of the next expression by assuming the surface temperature around the test heater to be uniform. The equations below are the temperature distribution and the existing boundary conditions we have for the horizontal cylinder.

$$\frac{\partial T}{\partial t} = a \left(\frac{\partial^2 T}{\partial r^2} + \frac{1}{r} \frac{\partial T}{\partial r} \right) + \frac{Q}{\rho_h c_{ph}} \quad (3)$$

Boundary conditions are as follows,

$$\left. \frac{\partial T}{\partial r} \right|_{r=0} = 0, \quad -\lambda \left. \frac{\partial T}{\partial r} \right|_{r=d/2} = q \quad (4)$$

$$T_a = \frac{\int_0^R T(2\pi r) dr}{\int_0^R (2\pi r) dr} = \frac{2}{R^2} \int_0^R T r dr \quad (5)$$

The experiment was carried out as follows. First, a boiling process for degassing of the liquid used in the experiment was performed at least for 30 minutes. Then, the liquid was fully filled in the boiling vessel with the free surface only in the pressurizer and liquid feed tank. Liquid temperatures and pressures in the boiling vessel and in the pressurizer were separately controlled to realize the desired saturated condition. At pressures more than atmospheric one, the experimental conditions were controlled by increasing the liquid temperature, and the pressurization was carried out by the steam itself.

Pre-pressure on cylinder surface before each experimental running at atmospheric pressure was given to the surface of heater in the saturated liquid pool system for 30 s with quasi-steady-state increasing heat input. The pre-pressure with various hydrostatic pressures up to 1.2 MPa were provided using a booster pump.

Experimental running is executed from high-speed analog computer based on required experimental condition and on each exponential period, τ . A high-speed video camera system (1000 frames/s with a rotary shutter exposure of 1/10000 s) was used to observe the boiling phenomena and to confirm the start of boiling on the test heater surface. The high-speed video camera was started before the starting of a measurement. A video timer started simultaneously with the starting of measurement, and then the boiling phenomenon was recorded with the passage of time.

4. Results and Discussion

4.1 Experimental conditions

Pool boiling processes were performed on a 1.0 mm diameter gold horizontal cylinder in a pool of saturated FC-72 by the transient heat inputs (exponentially increasing heat inputs ranging from quasi-steady-state to rapid increasing ones). Measurements were taken for the exponential periods, τ , and in a wide range of system pressures from sub

atmospheric of 79.5 kPa to 1082.0 kPa. The exponential period, τ , which represents the increasing rates of heat input was ranged from 10 ms up to 20 s. Table 2 shows the experimental conditions that were provided in this investigation.

Table 2. Experimental conditions

Working fluid	FC-72 (saturated condition)
Pressure, P	79.5 kPa ~ 1082 kPa
Saturation temperature, T_{sat}	323.7 K ~ 422.9 K
Pre-pressure	0 ~ 1.2 MPa
Exponential period, τ	10 ms ~ 20 s

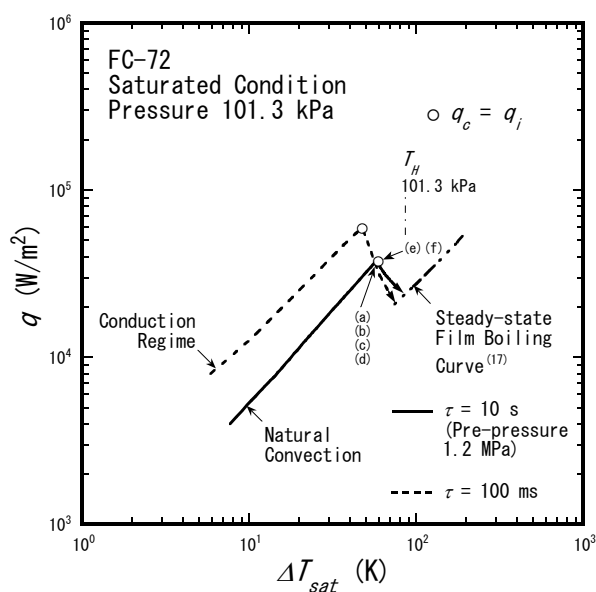


Fig. 2. Boiling heat transfer curves for direct transition boiling process

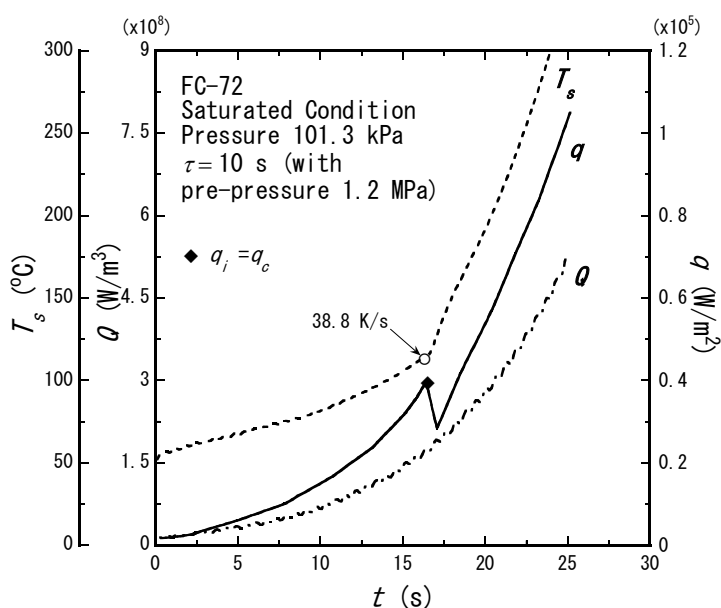


Fig. 3. Time dependence profile of q , Q , and T_s for direct transition (with pre-pressure of 1.2 MPa)

4.2 Direct transition boiling heat transfer process

Typical of boiling heat transfer processes on direct transition at CHF are shown on curves in Fig. 2, which represent characteristics of boiling heat flux, q , versus surface superheat, ΔT_{sat} . The curves for periods, τ , of 10 s and 100 ms that were measured at atmospheric pressure correspond to the quasi-steadily increasing heat input and rapidly increasing one, respectively. The applied pre-pressure of 1.2 MPa on measurement at $\tau=10$ s is the hydrostatic pressure added to the cylinder surface for a while prior to each experimental running to enable flooded cavities and to dissipate the activation of cavities for nucleate boiling by elimination of the possibility of entrapped vapor inside cavities.

It was observed that the direct transition process in the pool boiling of FC-72 predominantly occurs from the transient conduction process by rapid increasing heat input. In Fig. 2, a black dash line curve representing the direct transition at CHF for $\tau=100$ ms appears from increasing non-boiling conduction heat transfer up to the boiling inception and then followed by CHF simultaneously at surface heating rate of 3720 K/s, which results an equal value of incipient boiling and critical heat fluxes ($q_c=q_i$) at 6.0×10^4 W/m². The typical CHF and incipient boiling heat flux that were measured for the exponential period by rapid increasing heat input can be seen also in Figs. 7 and 8 for the graphs of q_c and q_i versus the periods, τ .

However, authors observed that the direct transition processes exist not only from conduction process but also from single phase natural convection. A same typical direct transition process has been confirmed to exist from quasi-steadily increasing natural convection on solid surface in the pool of FC-72 by measurements at around atmospheric and sub-atmospheric pressures, and by applied hydrostatic pressure or pre-pressure to the heater surface. In Fig. 2, it is represented by a black solid line curve for $\tau=10$ s with a given pre-pressure of 1.2 MPa. The curve has surface heating rate at the direct transition point at CHF, q_c , is 38.8 K/s and the value of q_c and q_i is 3.7×10^4 W/m². In the figure, it is seen also that the transition surface superheat of direct transitions in a pool of saturated FC-72 at atmospheric pressure is clearly lower than the corresponding homogeneous nucleation temperature, T_{Hn} , at 87 K, which was derived from Eq. (7) for predicting the homogeneous nucleation temperature near its spinodal limit as suggested by Lienhard⁽¹⁵⁾ (see § 4.7). The typical direct transition process at CHF is also represented by photographic observations shown in Fig. 4 that were taken at points (a) to (f) on the boiling curve for $\tau=10$ s (with a pre-pressure of 1.2 MPa) in Fig. 2.

Figure 3 shows graphs for the time dependence profile of q , Q , and T_s that were measured for period of 10 s, as a representation of direct transition boiling process due to quasi-steadily increasing heat input with a given pre-pressure of 1.2 MPa as seen in Fig. 2. In Fig. 3, although the surface heating rate is relatively low, it was observed that a direct transition process could exist without any occurrence of nucleate boiling from active cavities. It was assumed due to a kind of incipient boiling mechanism induced by the explosive-like HSN. After reached the CHF, q_c , the heat flux decreases down and almost reaches the corresponding minimum heat flux⁽¹⁶⁾ before finally enters the steady-state film boiling, while the surface temperature continues to increase (see also the reference of boiling curve in Fig. 2).

4.3 Photographic observations on vapor film behavior at direct transition

The corresponding phenomena of direct transition process that are shown in Figs. 4(a) to 4(f) start from a non-boiling regime of quasi-steadily increasing natural convection and proceed up to the incipient boiling point that is seen in the first photograph at point 4(a). A vapor film about 20 mm in length on the solid liquid contact appears at surface temperature of 387.74 K. Figures 4(a) to 4(d) show the vapor film behavior with a rapid growth of film covering the cylinder surface. Vapor film fully blankets the cylinder surface in only 3

ms from boiling incipience at point (a). It was assumed due to an explosive-like spontaneous nucleation (HSN) in originally flooded cavities on the cylinder surface and then forms the vapor tube concentrically covering the cylinder⁽¹⁾. Figure 4(e) was taken at 30 ms from point (a) just prior to the CHF and shows the detachment of bubbles from top of vapor tube which moves upward by buoyancy force from the position shown in the former photograph.

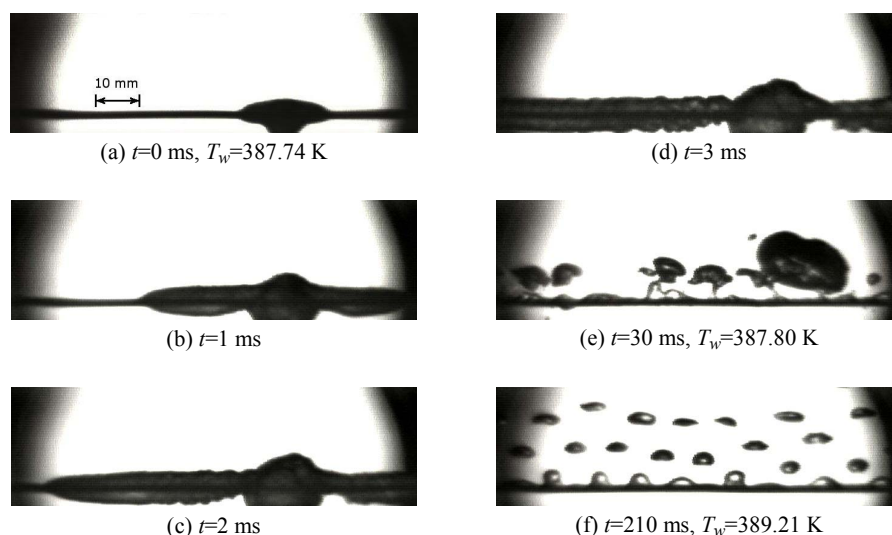


Fig. 4. Vapor film behaviors during direct transition to film boiling at 101.3 kPa under saturated condition for period of 10 s with a pre-pressure of 1.2 MPa

Direct transition occurs with a wavy pattern on vapor film surface. This process becomes significant and diminishes heat flux as the surface superheat increases. It was observed also that direct transition exists without boiling hysteresis or nucleate boiling occurrences as seen also on the boiling curve in Fig. 2. Transition boiling heat flux steeply decreases and almost reaches theoretical minimum film boiling at its contact interface temperature, T_i , which was suggested by Sakurai et al.⁽¹⁶⁾ (see § 4.7 and Eq. (9)). A thin, wavy vapor film continues to form while heat transfer process approaches the steady-state film boiling curve, which was derived from film boiling prediction by Sakurai et al.⁽¹⁷⁾. The facts of direct transitions at incipient boiling surface superheat confirm the assumption of the incipient boiling that is due to the explosive-like HSN in originally flooded cavities on cylinder surface at HSN surface superheat. Figure 4(f) at 210 ms from point (a) shows existing Taylor instability wave after detachment of bubbles and then continues to form new film boiling on the solid-liquid interface.

4.4 Effect of pre-pressure on direct transition boiling process

In the current work on horizontal gold wire, the incipient boiling surface superheats, ΔT_i , were measured by quasi-steady-state increasing heat inputs with periods, τ , of 10 s and by adding the pre-pressures up to 1.2 MPa in saturated pool of FC-72. As seen in Fig. 5, the incipient boiling superheats lie on a limit range of temperatures from 30 K to 60 K and seem to have a less dependence on the pre-pressure.

However, in higher pre-pressures, authors observed the spread of the potential incipient boiling superheats for dissipating nucleate boiling and inducing direct transition process. Figure 5 shows a constant boundary line at $\Delta T_i = 48$ K, which represents limit of incipient boiling surface superheat for inducing direct transition process. It divides the graph into region 1 and region 2 of ΔT_i for representing a different heat transfer process. The below region is the region 1 for ΔT_i with white circle marks that gives potential nucleate boiling

process from the cavities or nucleation sites on cylinder surface heater after the boiling incipience during transition to FDNB process. The above one is the region 2 for ΔT_i with black solid circle marks, which are followed simultaneously by CHF surface superheat for direct transition processes to film boiling. The ΔT_i for inducing FDNB processes appear up to pre-pressure of 1.0 MPa. However, the given pre-pressures of 1.2 MPa result the potential ΔT_i for fully direct transition processes with no FDNB processes. Another investigation on boiling inception in pool of FC-72 on horizontal platinum heater has been reported also by Mizukami et al.⁽¹⁸⁾ and observed a mechanism of incipient boiling process that was due to spontaneous nucleation and the incipient superheat was generally independent of the pre-pressure given to the solid surface.

The pre-pressure confirms also that quasi-steady-state heat transfer could induce a direct transition to film boiling at CHF. It gives an equal value of heat flux between the CHF, q_c , and the incipient boiling heat flux, q_i . These characteristics can be seen in Fig. 8 for graphs of q_c and q_i versus exponential periods, τ , that were measured at atmospheric pressure.

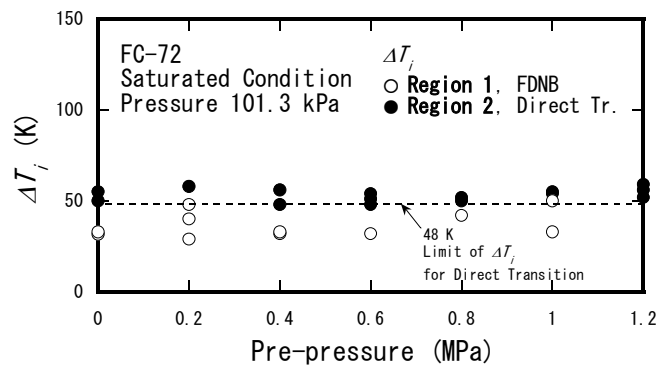


Fig. 5. Incipient boiling surface superheat vs. pre-pressure

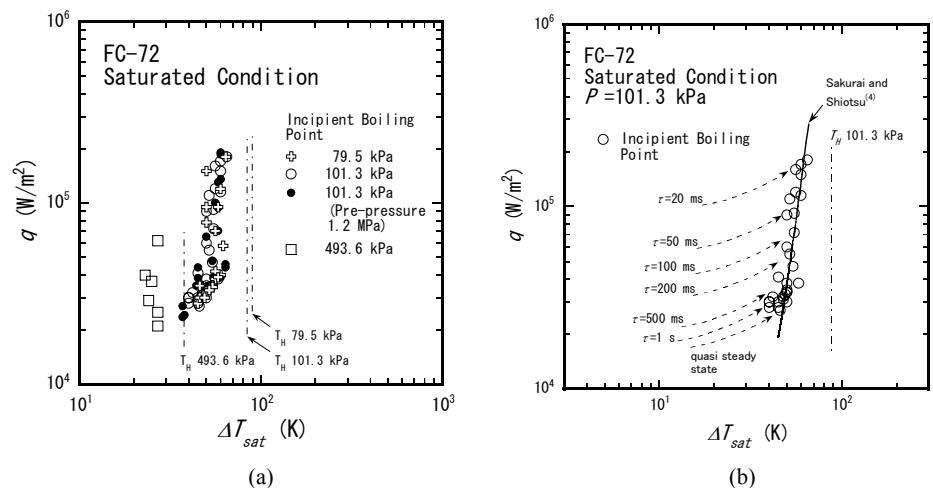


Fig. 6. Incipient boiling points for direct transition process

4.5 Incipient boiling surface superheat on direct transition at CHF

In Fig. 6(a), the incipient boiling points that are due to HSN for inducing direct transitions are shown on the graph of heat flux, q , versus surface superheat, ΔT_{sat} . They were measured for periods ranging from 10 ms to 20 s at a wide range of pressures. The incipient boiling surface superheat, ΔT_i , from both transient conduction and quasi-steadily increasing natural convection processes in non-boiling regimes for direct transition at CHF,

q_c , are lower than the values of homogeneous nucleation temperature, T_H .

At pressures of 79.5 kPa and 101.3 kPa, the direct transitions at q_c were derived from both transient conduction and natural convection processes by the rapid increasing heat inputs in short periods ($\tau \leq 500$ ms) and the quasi-steady-state increasing ones in long periods ($500 \text{ ms} < \tau < 20$ s), respectively. At heat fluxes below $4.5 \times 10^4 \text{ W/m}^2$, the q_c increase almost linearly with the increase in ΔT_i at each pressure. Those predominantly belong to direct transitions from natural convection by quasi-steady-state increasing heat inputs and a combine of transient conduction and natural convection, in a range of periods of $\tau > 500$ ms. However, at heat fluxes higher than around $4.5 \times 10^4 \text{ W/m}^2$, which exist from transient conduction and by rapid increasing heat inputs for periods of $\tau \leq 500$ ms, the q_c increase at an almost constant value of ΔT_i .

In Fig. 6(b), it is seen the incipient boiling points for direct transition process in saturated pool of FC-72 at atmospheric pressure. They were observed to exist at a range of periods, $10 \text{ ms} < \tau < 5$ s, by rapid increasing heat inputs and quasi-steady-state increasing ones. The incipient boiling points seem to have less dependence on the increasing rate of heating or decreasing rate of periods, τ , however, by shorter periods, the incipient boiling superheats are tending upward approaching the homogeneous nucleation temperature. The maximum heat fluxes or CHF for direct transition boiling processes at the incipient boiling points increase with the decrease in periods and agree with the corresponding curve obtained from the correlation that was suggested by Sakurai and Shiotsu⁽⁴⁾ (see the related explanation in § 4.6 below).

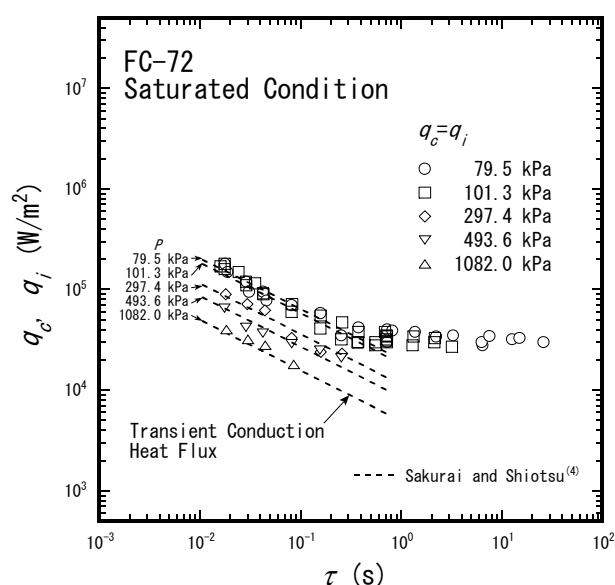


Fig. 7. CHF and incipient boiling heat flux for direct transition process

4.6 Transient CHF

The critical heat fluxes for direct transition process by transient heat inputs from quasi-steadily increasing heat inputs up to rapidly ones, were plotted on graphs of q_c and q_i for the exponential period, τ , in Figs. 7 and 8. They were measured under saturated conditions at a wide range of pressures from 79.5 kPa up to 1082.0 kPa and the exponential periods ranging from 10 ms up to 20 s.

In Fig. 7, the CHF, q_c , at pressures of 79.5 kPa, 101.3 kPa, 297.4 kPa, 493.6 kPa, and 1082 kPa were plotted for periods, τ . On the direct transition, the CHF occurs simultaneously after the incipient boiling, thus it has equal value with the incipient boiling heat flux, q_i , which were plotted in same marks with the CHF at every pressure. Ones

observed the direct transitions at CHF at pressure of 79.5 kPa were obtained not only from non-boiling transient conduction but also single phase natural convection. They appear in whole range of short periods of $\tau \leq 1000$ ms and even in quasi-steadily and steady-state ones at $\tau > 1000$ ms and $\tau \geq 20$ s, respectively. The q_c in quasi-steady-state periods up to steady-state show almost a constant value. On the other hand, the q_c in short periods increase with the decrease in periods. Measurements at atmospheric pressure also result direct transitions from quasi-steady-state increasing heat input up to periods of $\tau < 5$ s.

At higher pressure than atmospheric, the direct transitions appear predominantly in shorter periods of $\tau < 300$ ms from transient conduction by rapid increasing heat inputs. Within short periods, the q_c increase with the decrease in periods, and the period of the minimum CHF at each pressure shortens with the increase in pressure. The possible of nucleate boiling processes in the short periods or by rapid increasing heat inputs were observed to exist at higher pressures. It was assumed that boiling process at high pressure near its homogeneous temperature makes it possible for inducing an insufficient HSN process and then initiates nucleate boiling without the direct transition boiling process to film boiling.

In Fig. 7, the CHF for direct transition boiling process at short periods of $\tau < 1000$ ms are dependent on pressure. This phenomenon can be expressed by the corresponding value of CHF for periods in linear asymptote lines that were plotted in Fig. 7 by black dash lines. The corresponding lines were obtained from a correlation in terms of non-boiling heat transfer coefficient from transient conduction process that was suggested by Sakurai and Shiotsu⁽⁴⁾, that is, $q_c = h_c \Delta T_i(\tau)$ for saturated condition, where $h_c \equiv (k_i \rho_i c_{pi} / \tau)^{0.5}$. The conduction heat transfer coefficients, h_c , by exponentially rapid increasing heat inputs were observed to increase rapidly with the decrease in τ and approach a certain asymptotic value.

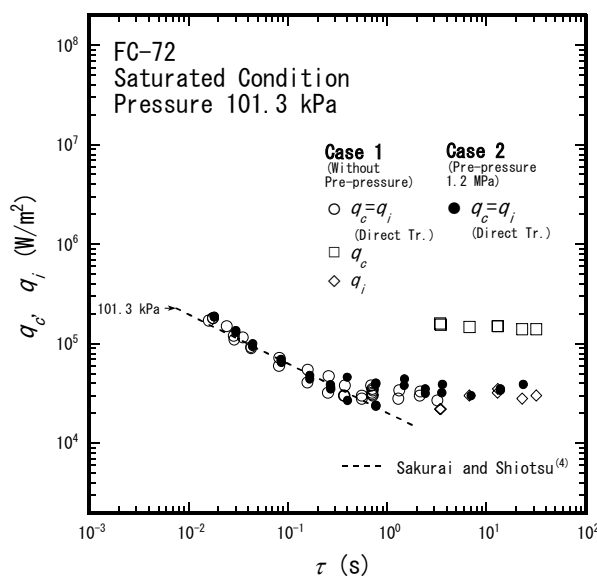


Fig. 8. Effect of pre-pressure on CHF and incipient boiling heat flux for direct transition process

Figure 8 shows the effect of pre-pressure on the CHF for direct transition process to film boiling. It is shown on graph of q_c and q_i for the period, τ , on measurements of case 2 with pre-pressure of 1.2 MPa at atmospheric pressure under saturated condition. The case 1 of q_c for direct transitions without pre-pressure is also plotted as a comparison. In case 1 without pre-pressure, the boiling heat transfer at quasi-steady-state periods, $\tau > 3$ s, gives CHF at the transition from fully development nucleate boiling (FDNB) to film boiling that was assumed due to the hydrodynamic instability (HI). It gives an almost constant of q_c at

average value of $1.5 \times 10^5 \text{ W/m}^2$, which are plotted on graph with hollow square marks. From the observations of boiling phenomena by photograph and high speed video, it was observed that the FDNB process is induced by the activation of cavities entraining vapor after detachment of bubbles from top of vapor film covering cylinder surface. It was observed to occur during the incipient boiling process, which is followed by boiling hysteresis with rapid change of heat flux and surface superheat just prior to detachment of bubbles. The incipient boiling heat fluxes, q_i , belong to case 1 were plotted on graph by white diamond marks.

As seen in Fig. 8, the measurements with pre-pressure 1.2 MPa in case 2 give the direct transitions at CHF from not only transient conduction in short periods by rapid increasing heat input but also from natural convection in long periods by quasi-steadily increasing heat inputs, and result an equal value of q_c and q_i from simultaneously process of incipient boiling and CHF. The q_c and q_i were plotted with same solid black circle marks. The CHFs, q_c , from transient conduction heat flux in short periods of $\tau \leq 1000 \text{ ms}$ increase with the decrease in periods. However, during quasi-steady-state periods up to steady-state ones at $\tau > 1000 \text{ ms}$, the q_c approach a constant value at around $3.5 \times 10^4 \text{ W/m}^2$. Compared to the CHF in case 1 for quasi-steady-state periods, the effect of pre-pressure on CHF in the case 2 shows a quite different phenomenon.

The values of CHF belong to direct transitions in case 2 by quasi-steady-state increasing heat inputs are about 77% lower than ones in the case 1 belong to CHF from FDNB process. However, on both cases 1 and 2, the direct transitions from transient conduction by rapid increasing heat inputs within short periods show a same typical increasing rate of CHF that increase with the decrease in periods, and can be expressed by the corresponding linear asymptote line.

4.7 Predictions of incipient boiling surface superheat and CHF for direct transition boiling process

A bunch of predictions of CHF for boiling heat transfer has been reported in literatures. However the preceding prediction of CHF should be credited to Kutateladze⁽¹⁹⁾ and Zuber⁽²⁰⁾ for their hydrodynamic instability analysis. In the transient boiling heat transfer with a wide range of exponential periods under various pressures and liquid subcoolings, it was suggested that the CHF could be explained by the HSN model at its lower limit superheat instead of the hydrodynamic instability (HI) model^(1-3, 9, 10). In the current work, direct transition process by exponentially rapid increasing heat inputs at short periods of $\tau < 1000 \text{ ms}$, the CHF and its mechanism for transition boiling from non-boiling to film boiling were confirmed due to the heterogeneous spontaneous nucleation with an explosive-like boiling inception and then followed by CHF simultaneously to proceed the transition boiling. This kind of transition boiling phenomenon shows a significant correlation of the boiling inception and CHF mechanisms.

The prediction of CHF by exponentially increasing heat input has been suggested by Sakurai and Shiotsu⁽⁴⁾ for the correlation of the heat flux at the incipient boiling superheat with predominant heat transfer coefficient from transient conduction process. The heat flux is maximum heat flux or CHF, q_c , and is equal with the incipient heat flux, q_i , for direct transition process. This correlation could explain the phenomena of direct transition process by rapid increasing heat input at short period region and shows well agreement with the experimental data as seen in Figs. 6(b), 7, and 8.

In Fig. 9(a), the current data of CHF, q_c , and incipient boiling heat flux, q_i , from direct transition boiling process on 1.0 mm horizontal gold cylinder at the representation of short periods of 20 ms and 100 ms by rapid increasing heat inputs and at quasi-steady-state periods of 10 s and 20 s were plotted for the reduced pressure, P/P_{CR} . Other data from measurements by transient heating on different horizontal geometry and material of the

heater were also plotted. It shows that the increasing rates of q_c and q_i at short periods increase non-linearly with the decrease in reduced pressure. The heat flux also significantly depends on the rate of the exponential period, τ , at each pressure, which is also shown by the typical heat flux for period in Figs. 6(b), 7, and 8. However, direct transition processes from natural convection at steady-state periods of 10 s and 20 s for pressures of 79.5 and 101.3 kPa seem to give q_c with a constant of increasing rate.

$$q_c(\tau) = A(P/P_{CR})^{-0.5} \quad (6a)$$

$$\Delta T_i(\tau) = B(P/P_{CR})^{-0.5} \quad (6b)$$

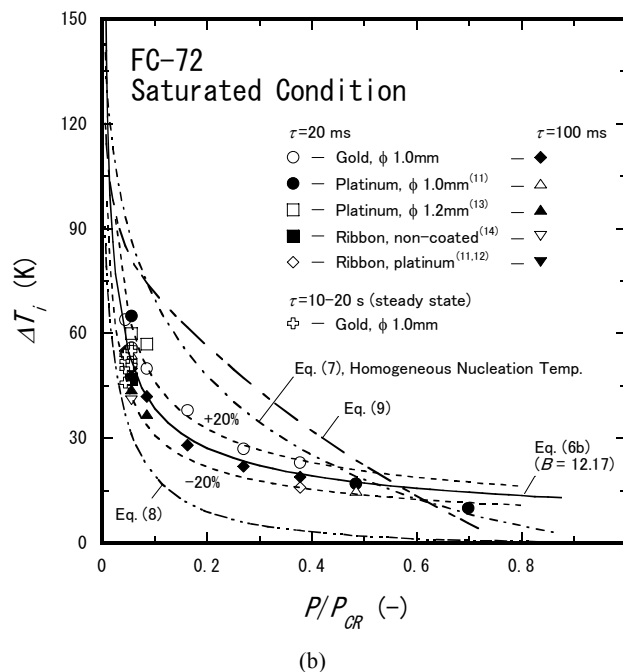
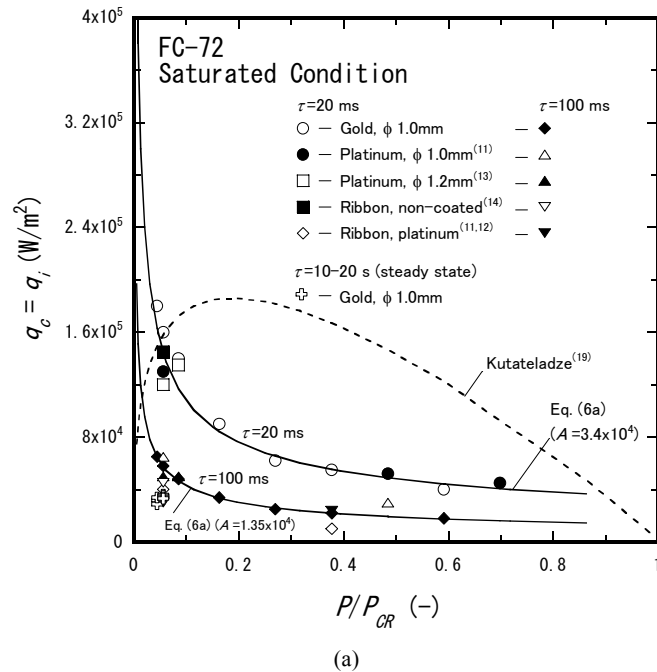


Fig. 9. (a) q_c , and (b) ΔT_i vs reduced pressure

In order to express the typical increasing rate of CHF for direct transition at short periods by rapid transient heat transfer, a corresponding curve in black solid lines derived from Eq. (6a) was plotted in graph based on the experimental data. The empirical correlation in Eq. (6a) is proposed to predict the corresponding CHF and incipient heat flux, q_c and q_i , for the direct transition process by rapid increasing heat inputs at short periods of τ . It is a function of the non-dimensional parameter of the reduced pressure, P/P_{CR} , to the power of -0.5 to express non-linearly the increasing rate of CHF, and a constant, A , which was obtained from least square fit to experimental data. The corresponding curve shows a good agreement with the experimental data at each of short periods for various reduced pressures, with constants A are equal to 3.4×10^4 and 1.35×10^4 for periods of 20 ms and 100 ms, respectively. The corresponding curve for steady state CHF by HI model was also plotted for comparison from Kutateladze's correlation⁽¹⁹⁾.

One of important mechanisms in the boiling heat transfer process and should be responsible for occurring spontaneous nucleation is the incipient boiling process. The boiling inception model at certain required superheat limit is important to be quantified for its prediction and accuracy of evaluation on boiling heat transfer system. The predictions of the incipient boiling superheat have been suggested to include the homogeneous nucleation temperature, T_H , close to the thermodynamic spinodal limit, which was suggested by Lienhard⁽¹⁵⁾ in Eq. (7). Moreover, in the prediction of incipient boiling superheat for engineering approximation, it mostly takes account the heterogeneous nucleation superheat. In the pool boiling of highly wetting liquid, the prediction of heterogeneous nucleation superheat often involves the phenomena of boiling hysteresis before the onset of nucleate boiling, which considers the effect of surface tension and the prediction of effective radius of vapor bubble on surface including the Rohsenow's estimation for fully developed nucleate boiling, as seen in Eq. (8)⁽²¹⁾ for the prediction of the incipient boiling hysteresis ΔT_{IBH} . In the heterogeneous spontaneous nucleation, prediction of incipient boiling superheat as the lower limit HSN superheat may also refer to the contact interface temperature of cylinder surface, T_I , which closely agrees with the minimum film boiling temperature, as suggested in Eq. (9) by Sakurai et al.⁽¹⁶⁾.

$$T_{sp} - T_{sat} \cong T_{CR} \left[0.923 - \frac{T_{sat}}{T_{CR}} + 0.077 \left(\frac{T_{sat}}{T_{CR}} \right)^9 \right] \quad (7)$$

$$\Delta T_{IBH} = T_{sat}(P_v) - T_{sat}(P) - C(q_i)^b; \text{ where } P_v = P + \frac{2\sigma}{r} - P_{gas} \quad (8)$$

$$\Delta T_I = T_I - T_{sat}; \text{ where } T_I = 0.92T_{CR} \left\{ 1 - 0.26 e^{\left[\frac{-20(P/P_{CR})}{1+1700/P_{CR}} \right]} \right\} \quad (9)$$

However, in the boiling heat transfer phenomena by rapid exponentially increasing heat inputs with short periods of $\tau < 1000$ ms for a wide range of pressures, the mechanism of incipient boiling that is assumed due to spontaneous nucleation contributes significantly the initiation process of boiling for inducing the direct transition to film boiling. In the pool of saturated FC-72, the incipient superheats, ΔT_i , have been measured for a wide range of system pressures up to 1082 kPa and were plotted in graph for the reduced pressure, P/P_{CR} , as seen in Fig. 9(b). The current data for 1.0 mm diameter horizontal gold cylinder by quasi-steady-state increasing heat inputs at periods 10 s and 20 s, and by rapid increasing ones at short periods of 20 ms and 100 ms were plotted in the figure with bold plus, white circle, and black solid diamond marks, respectively. The ΔT_i for short periods increases non-linearly with the decrease in reduced pressures and approaching the homogeneous nucleation temperature. These data were accompanied also for comparison by other measured data with transient heating from different horizontal geometries and materials of

heaters. However, the incipient surface superheats seem to have less dependence on the exponential periods, τ , at each pressure.

This typical incipient boiling superheat for direct transition process by rapid increasing heat input at short periods can be also predicted by a corresponding non-linear curve on solid line plotted in the figure. It was obtained from the empirical correlation in Eq. (6b) as a function of non-dimensional parameter of the reduced pressure, P/P_{CR} , and a constant, B , which is the corresponding value of incipient boiling superheat and was obtained from least square fit to the experimental data. As seen in the figure, the corresponding curve almost agrees with the measured data, which are lying within an error range of $\pm 20\%$, with $B=12.17$. The other predictions of incipient boiling superheat were also plotted for comparison, which were calculated from Eqs. (7-9) and based on the corresponding saturation temperature. The incipient boiling superheats for a wide range of system pressures are mostly lower than the homogeneous nucleation temperature. In Fig. 9(b), the curve of ΔT_{IBH} from Eq. (8) was obtained without taking into account the third component in the equation for Rohsenow's estimation of FDNB in the boiling hysteresis and then remains the first and second components, which reserve as the incipient boiling superheat in the heterogeneous nucleation process. In this calculation, the radius of cavity or the effective radius of vapor bubble embryo on surface, r , was using a fixed value of $0.1 \mu\text{m}^{(22)}$.

5. Conclusions

The direct transition processes from non-boiling to film boiling in a pool of saturated FC-72 by exponentially increasing heat inputs were investigated in a wide range of pressures and exponential periods. The direct transition processes were observed predominantly to occur from non-boiling regime of transient conduction by rapid increasing heat inputs. However, the investigation also observed ones from natural convection by quasi-steadily increasing heat inputs.

The direct transition at CHF confirmed a kind of incipient boiling process that was due to heterogeneous spontaneous nucleation in originally flooded cavities on cylinder surface without nucleate boiling occurrences. It was confirmed also by adding a pre-pressure on surface at atmospheric pressure during quasi-steady-state increasing heat input, which observed the incipient boiling process from an explosive-like HSN and then induced direct transition from single phase natural convection rather than transient conduction. However, the direct transition from natural convection by quasi-steady-state increasing heat input at atmospheric pressure, gave the values of CHF 77% lower than ones in the case without pre-pressure from a FDNB process. The direct transitions at CHF from natural convection were also observed in measurements on saturated FC-72 under sub atmospheric pressure.

The direct transition phenomena at CHF from transient conduction by rapid increasing heat input were significantly dependent on pressure and can be expressed by the corresponding asymptote values of CHF for short periods. Effective prediction for the phenomena was also figured by typical incipient boiling surface superheat, ΔT_b , and the CHF, q_{cs} , in the empirical correlations in Eqs. (6a) and (6b) for a function of the variable reduced pressure, P/P_{CR} , and the corresponding constants, A and B , which are required to express each rate at period, τ .

References

- (1) Sakurai, A., Mechanism of Transitions to Film Boiling at CHF's in Subcooled and Pressurized Liquids Due To Steady and Increasing Heat Inputs, *Nuclear Engineering and Design*, Vol. 197 (2000), pp. 301-356.
- (2) Sakurai, A., Shiotsu, M., and Hata, K., Boiling Heat Transfer from a Horizontal Cylinder in

- Liquid Nitrogen. *ASME-HTD In: Kelley, J.P., Superczynski, M.J. (Eds.), Heat Transfer and Superconducting Magnetic Energy Storage*, Vol. 211 (1992), pp. 7–18.
- (3) Fukuda, K., Liu, Q., Park, J., and Kida, H., Pool Boiling Critical Heat Flux of Highly Wetting Liquid, *Journal of the JIME*, Vol. 39, No. 10 (2004), pp. 25-32.
 - (4) Sakurai, A., and Shiotsu, M., Transient Pool Boiling Heat Transfer, Part 1: Incipient Boiling Superheat, *ASME J. Heat Transfer*, Vol. 99 (1977), pp. 547-553.
 - (5) Okuyama K., Mori S., Sawa K., and Iida Y., Dynamics of Boiling Succeeding Spontaneous Nucleation on a Rapidly Heated Small Surface, *International Journal of Heat and Mass Transfer*, Vol. 49 (2006), pp. 2771-2780.
 - (6) Avksentyuk, B.P., Kravchenko, V.M., Ovchinnikov, V.V., and Plotnikov, V.YA., Study of the Shape of Vapor Formations in Explosive Boiling, *Heat Transfer Research*, Vol. 38, No. 3 (2007), pp. 223-232.
 - (7) Shepherd, J.E., and Sturtevant, B., Rapid Evaporation at the Superheat Limit, *Journal of Fluid Mechanics*, Vol. 121 (1982), pp. 379-402.
 - (8) Nghiem, L., Merte, H., Winter, E.R.F., and Beer, H., Prediction of Transient Inception of Boiling in Terms of a Heterogeneous Nucleation Theory, *Journal of Heat Transfer*, Vol. 103 (1981), pp. 69-73.
 - (9) Sutopo, P. F., Fukuda, K., and Liu, Q., and Park J., Transient Pool Boiling Critical Heat Flux of FC-72 Under Saturated Conditions, *JSME Journal of Power and Energy Systems*, Vol. 1 No.2 (2007), pp. 178-189.
 - (10) Sutopo, P. F., Fukuda, K., and Liu, Q., Transient Critical Heat Fluxes in Subcooled Pool Boiling of FC-72, *JSME Journal of Power and Energy Systems*, Vol. 2 No.2 (2008), pp. 804-814.
 - (11) Sutopo, P. F., Pool Boiling Heat Transfer Phenomena on Horizontal Geometries in FC-72, *Master Thesis* (2008), Kobe University.
 - (12) Sutopo, P. F., Fukuda, K., and Liu, Q., Transient Pool Boiling CHF in FC-72, *Proceedings of 2008 ASME Summer Heat Transfer Conference*, CD-ROM, HT2008-56272 (2008), pp. 1-17.
 - (13) Kasakawa, T., Hata, K., and Shiotsu, M., Transient Heat Transfer on a Horizontal Cylinder in FC-72, *Advances in Electronic Packaging*, Vol. 26-2 (1999), pp. 1471-1478.
 - (14) Ohya, M., Hata, K., Shiotsu, M., Transient Heat Transfer from a Flat Plate in a Pool of FC-72, *Proceedings Of IPACK'01 – The Pacific Rim / ASME International Electronic Packaging*, IPACK2001-15575 (2001), pp. 753-761.
 - (15) Lienhard, J.H., Corresponding States Correlations of the Spinodal and Homogeneous Nucleation Limits, *Journal of Heat Transfer*, Vol. 104 (1982), pp. 379-381.
 - (16) Sakurai, A., Shiotsu, M., and Hata, K., Effect of System Pressure on Minimum Film Boiling Temperature for Various Liquids, *Experimental Thermal and Fluid Science*, Vol. 3 (1990), pp. 450-457.
 - (17) Sakurai, A., Shiotsu, M., and Hata, K., A General Correlation for Pool Film Boiling Heat Transfer from a Horizontal Cylinder to Subcooled Liquid, Part 2: Experimental Data for Various Liquids and Its Correlation, *ASME J. Heat Transfer*, Vol. 112 (1990), pp. 441–450.
 - (18) Mizukami, K., Hara, K., Mukasa, S., and Abe, F., Boiling Inception on Platinum Surface in FC-72 (2) (Effect of Pressure) (In Japanese), *HTSJ 42nd National Heat Transfer Symposium (2005-6)*, Paper No. E223 (2005), pp. 279-280.
 - (19) Kutateladze, SS., Heat Transfer in Condensation and Boiling, *AEC-tr-3770* (1959), USAEC.
 - (20) Zuber, N., Hydrodynamic Aspects of Boiling Heat Transfer, *AECU-4439* (1959), USAEC.
 - (21) Bar-Cohen A. and Simon T.W., Wall Superheat Excursions in The Boiling Incipience of Dielectric Fluids, *Heat Transfer Engineering*, Vol. 9 No. 3 (1988), pp. 19-31.
 - (22) Sutopo P. F., Fukuda, K., and Liu, Q., Photographic Study on Transient Pool Boiling Phenomena in FC-72, *Proceedings of 77th JIME Annual Meeting*, Paper No. 218 (2007), pp. 81-82.